

The impact of Hurricane Katrina on the New Orleans urban heat island

Aram Parrish Lief¹
Mahtab Ahmed Lodhi¹

¹ University of New Orleans - UNO
Lakeshore Drive - 2000 - 70148 - New Orleans - LA, USA
aplief@uno.edu, mlodhi@uno.edu

Abstract. Due to its location at the Mississippi River Delta next to two large water bodies, several tropical cyclones and floods have impacted the City of New Orleans for over two centuries, some of which caused widespread degradation of the urban ecosystem. In 2005, Hurricane Katrina's diverse impacts included damaged and destroyed trees, and other despoiled vegetation, which also increased the exposure of artificial and bare surfaces, known drivers that contribute to urban heat island (UHI). Unlike previous studies that focused on sprawl and the slow intensification of anthropogenic activities as the causes for increased UHI effect, the purpose of this study was to determine if a natural phenomenon altered its pattern and intensity. A time series of enhanced Landsat TM imagery was used to show the impact of an extreme weather event on the pattern and intensity of UHI. Using pixel-based classification and change detection methods, land surface temperature (LST) retrieval, and field data, the authors found a measurable change in the pattern and increased intensity of the New Orleans UHI effect. The hottest LST pixels (36°C and higher) dramatically increased in surface area from 60.15 km² to 111.24 km², which occurred from the year 2003 to 2005. This finding may be relevant to urban planners and stakeholders regarding future natural disasters and other human impacts.

Keywords: land surface temperature, tropical cyclones, Landsat TM, image processing, remote sensing.

1. Introduction

This study investigated the climatic phenomenon known as the *urban heat island* (UHI) in the aftermath of Hurricane Katrina, which severely impacted the Greater New Orleans (GNO) area in 2005. It entailed the analysis of pre- and post-storm Landsat-5 Thematic Mapper (TM) imagery, including changes to surface heat patterns, vegetative cover and the abrupt alteration of its UHI. Like previous research, this study focused on land cover-temperature relationships, but it differs in that we hypothesized that natural forces could also cause a change in thermal pattern and intensity, and over a very short period of time. UHIs are typically measured at the local or mesoscale, from 10² to 10⁴ meters (Oke 1982). Three different types of UHIs are defined according to methodological approach, instrumentation, and data: 1) atmospheric; 2) subsurface; and 3) surface. This study examined the UHI effect on the GNO area based on satellite-derived surface temperature measurements.

Understanding the UHI phenomenon and its impacts on human health and urban environments is important to policymakers and stakeholders, and it should be regarded as an integral component to the study of the urban ecosystem complex. UHI is directly linked to concerns such as, heat-related illnesses, air pollution, energy conservation, urban beautification, and the need for the conservation and creation of urban green spaces. Another rationale is the fact that a comprehensive UHI study of New Orleans had never been done before, nor had any UHI studies examined the impact of rapid loss of vegetative cover on the UHI of a coastal city when this study began. Previous studies utilizing remote sensing techniques have addressed the impact of hurricanes on wetlands and forests in coastal regions (Cablak et al. 1994). However, there remains a dearth of studies regarding the possible linkages between catastrophic storms, and other natural disasters, and the alteration of the UHI effect of coastal cities.

Hurricane Katrina caused unprecedented destruction and degradation of the urban ecosystem, inflicting serious damage to city's extensive and dense cover of large, old growth shade trees. Therefore, any likely thermal variation triggered by dramatic perturbation of city's natural landscape should have measurable consequences in the form of higher sensible heat

with a unique distribution and pattern of hot spots within the study area. The rapid and extensive loss of vegetative cover is a variable that, it was assumed, had significantly affected the pattern, distribution, and intensity of the UHI effect. Therefore the objective of this study was to answer fundamental questions regarding the state of the vegetative cover before and after the hurricane, and how it affected the pattern and intensity of heat distribution throughout the study area. The following hypotheses were tested: 1) the loss and re-growth of vegetation after hurricane Katrina altered the UHI; and 2) Post-hurricane re-growth of vegetation has occurred in the same locations of significant loss, thus following the historical, pre-established pattern of urbanization.

1.1 Study area

The largest city in the State of Louisiana, New Orleans is located in the Lake Pontchartrain Basin, the world's fourth largest drainage basin in the seventh largest delta. The Mississippi River and its natural levees bisect the City from west to east. A complex system of canals, some of which are perpendicular to the River and Lake Pontchartrain to the north, allow for drainage whenever there is citywide flooding. Since the majority of the City lies below sea level, it is protected by flood walls that reach up to nearly 10 meters high, and natural levees that are at approximate 5 meters above mean sea level. 80 percent of the City was affected by persistent flooding after Katrina, which remained for approximately five weeks, depending on the neighborhood and depth of elevation.

The climate of New Orleans and the surrounding region is influenced by its subtropical latitude, and its proximity to the Gulf of Mexico, which results in milder winters than inland areas. The average annual temperature in New Orleans is 19.9° Celsius (C), and daily average temperature ranges from 11.9° C in January to 28.5° C in July. Heat index calculations are often higher than 40° C on very hot and humid days, and during winter the temperature normally remains above freezing. Louisiana is the wettest state with a total yearly precipitation of 158.62 centimeters (cm), and monthly extremes averaging 45.63 cm. Frequent and sometimes heavy rains occur in the GNO area causing floods every year. Tropical systems are common in the northern part of the Gulf of Mexico, with cyclogenesis occurring typically below 25° degrees north latitude. Hurricanes spawn tornadoes and create storm surges that flood coastal and inland areas with salt water. Flooding is a major hazard produced by rainfall and the storm surge, which can exceed 7 meters (m) in extreme cases.

The geographic extent of the study area covered the GNO metropolitan area (29°51'N to 30°03'N, 89°54'W to 90°18'W) where there is a reasonable delineation between the built and non-built environment. The area of interest (AOI) is approximately 530 square kilometers (km), excluding the river that bisects it, and the distance from west to east is approximately 40 km, and north to south 25 km. Since this study focused on determining the impact of a tropical cyclone on the GNO area, it was necessary to collect data imagery *before* and *after* the weather event, and after a period of vegetative regrowth had occurred.

2. Methods

2.1 Data and preprocessing

Landsat TM data imagery were used to derive land surface temperature, land cover classifications, and spectral indices in order to indicate the changes to the local UHI using change detection techniques, with knowledge that the sensor has well-known spatial and radiometric limitations. Moreover, it should be noted that using LST as a measure of UHI has several methodological, technical, and logistical limitations. We collected cloud-free TM data starting with October 1987 until September 2011. This allowed for an attempt to capture the more subtle effects of hurricane Andrew (1992), and hurricanes Isadore and Lili (2002), as they did not impact the City nearly as much as Katrina. Of the one hundred and twenty-seven

TM images that were collected, thirty-two were used. Often the best satellite images for Southeastern Louisiana are captured around mid-Fall (September to October). A few ETM+ scenes were used with field data for validation purposes. ASTER NDVI emissivity values for the AOI were collected for input into the Landsat TM LST retrieval model. Climate reports were obtained from the National Climatic Data Center (NCDC). National Weather Service (NWS) COOP weather station data were compared with the mobile weather data, which were collected using weather sensors mounted on a vehicle at screen height (~2 m). Air temperature, relative humidity, and skin temperature data were collected along several transects throughout the entire City, and at the urban-rural fringe. These data were used to compare to surface temperature results derived from the Landsat data, and to characterize the ground level distribution of heat.

Pre-processing of the Landsat images included, layer stacking (combining the separate bands of data imagery into one file), radiometric normalization (to account for solar angle and atmospheric effects), image sub-setting (clipping the AOI from the entire scene), and a gap-filling technique used for the ETM+ images for visualization purposes. The image-based, absolute radiometric correction method, *dark object subtraction* (DOS) was used for atmospheric correction of TM bands 1-5,7 based on Chavez (1996) *cosine of the solar zenith angle* (COST). A vector-based shape file of the AOI was used to *subset*, clip out the AOI from Landsat scenes. Water was masked through the subset process, including the Mississippi River, larger canals, and small lakes and ponds. If any canal was 30 m or less, it was not clipped due to pixels mixed with land features. LST was derived from TM thermal band 6 using a single channel algorithm (Yuan and Bauer 2007; Sobrino et al. 2004) to convert top of atmosphere (TOA) brightness temperature to surface temperatures, which required four parameters: 1) transmittance; 2) upwelling; 3) downwelling; and 4) emissivity. The first three parameters were obtained from MODTRAN using four user inputs: 1) temperature; 2) relative humidity; 3) elevation; and 4) barometric pressure. The fourth value, emissivity, was derived from the ASTER spectral library Version 2.0. Since heterogeneous surfaces, and thus mixed pixels of vegetation and urbanized surfaces, are highly prevalent in the AOI, emission values along two transects of the AOI were extracted from the ASTER image, and then averaged to 0.975 (Jiménez-Muñoz et al. 2006).

2.2 Spectral computations and change detection

The *unsupervised* classification approach was chosen for this study due to the highly heterogeneous terrain of the AOI, utilizing the K-means statistical clustering algorithm in an *Iterative Self-Organizing Data Analysis* (ISODATA) mode. ISODATA was used to develop thematic-based temperature maps based on the TM thermal band 6, which underwent several phases of corrections and enhancements in order to create an LST time series. Land cover classifications were based on the remaining bands (1-5,7). In this study, four spectral indices, two slope-based vegetation indices, a moisture index, and a water index were tested to perform land cover analysis. The Normalized Difference Vegetation Index (NDVI) is often utilized to represent vegetation, however, this study also tested the Modified Soil-Adjusted Index (MSAVI), the Normalized Difference Moisture Index (NDMI), and the Modified Normalized Difference Water Index (MNDWI) to see which could better enhance vegetation and tree canopy, leaf moisture content, and which had better separation from other features. After carefully evaluating the outcome of the other indices, it was decided to use only NDVI in the final land cover analysis. Tasseled Cap Transformation (TCT) method was used to compress the raw image bands into components related to class types: *brightness* (TC1), *greenness* (TC2), *yellowness* (TC3), and *nonessuch* (TC4), the last being related to senescent vegetation and atmospheric conditions, which was not used. The TCT enhanced images were used in the experimental, compound indices, and also for composite images used for change detection.

Accuracy assessments were performed on the transformed data imagery employing an error matrix to measure percentage of omission and commission of error, overall classification accuracy, and Cohen's Kappa coefficient. Weather and climate data, field data, and visual analysis of the classified images was performed, procedures commonly used in studies based on satellite imagery analysis (Foody 2002). A priori knowledge of the image coverage area was useful during this process. 0.3-meter panchromatic High Resolution Orthoimagery (HRO) using the ADS40 sensor, 1-meter Digital Ortho Quarter Quads (DOQQs) orthoimagery, and color infrared (CIR) National High Altitude Photography (NHAP) were available for some years critical to this study.

Two methods were used for measuring change to LST. First, histograms of LST images were compared, and then differenced through image subtraction. The results were examined at different scales, based on physical, political, and cultural boundaries. The second was the post-classification method applied to LST images using the ISODATA algorithm. This alternative approach enabled change detection to be accomplished via automatic, objective pattern recognition. Both of these LST image products were used together with ancillary data in order to examine the LST patterns within the AOI. Anthropogenic and natural impacts on urban vegetation were also examined using spectral indices with the LST products. Temperature values were replaced by six levels or classes of temperature. After the ISODATA classification program finished, the six classes were color coded, compared to the LST images, given subjective descriptions, then an index was created based on comfort stress levels. Finally, a change detection method was applied to the spectrally enhanced images called the RGB method, which is often used with NDVI (RGB-NDVI). An advantage of this method is that it utilizes three dates instead of two, eliminated the need for setting a threshold levels of change, and reduced processing steps (Wilson and Sader 2002; Sader et al. 2003)

3. Results and discussion

The change in pattern and intensity of LST was apparent upon first visual inspection of the images. After the LST images were normalized to a middle date, the grayscale rasters were displayed in a viewer as pseudo-color images, and then color coded according to the six discrete classes. LST images were subtracted and the changes color coded. The results indicate a slight trend until the Hurricane Katrina event. Then there is a successive, doubled increase for the next three images, the latter of which was captured after Hurricane Gustav (2008), and then a net decrease in LST from October 2008 to October 2010. The changed surface areas were calculated from pixels of 10% increase and 10% decrease, from a total area (AOI) of approximately 1342.1 km². In the areas where LST increase is clustered, there were significant changes to the surface features, such as damage to urban forests. Higher temperatures were recorded over most areas that were flooded for several days. Some of the highest temperatures were clustered in areas where the flood water remained for several weeks. Constant flux was observed in all of the neighborhoods and districts within the AOI, however persistent patterns were also observed, indicating hot and cool spots or *microclimates*. In order to quantify these patterns, the images were reviewed and several locations were chosen for further examination, which included neighborhoods, planning districts, shopping areas, playgrounds and parks.

The LST images were classified using the unsupervised ISODATA algorithm into thematic-oriented discrete comfort classes described above. In order to detect change between the different years, the thematic layers created from the ISODATA process were fused into a matrix where the classes of the two input layers (year 1 and year 2) represent the rows and columns of the matrix. The resultant classes were derived from the coincidence of any two input classes, unique for each coincidence of two input class values, and the background was assigned 0. Figure 1 below shows the surface heat pattern and intensity of the New Orleans UHI effect from before and after the impact of Hurricane Katrina.

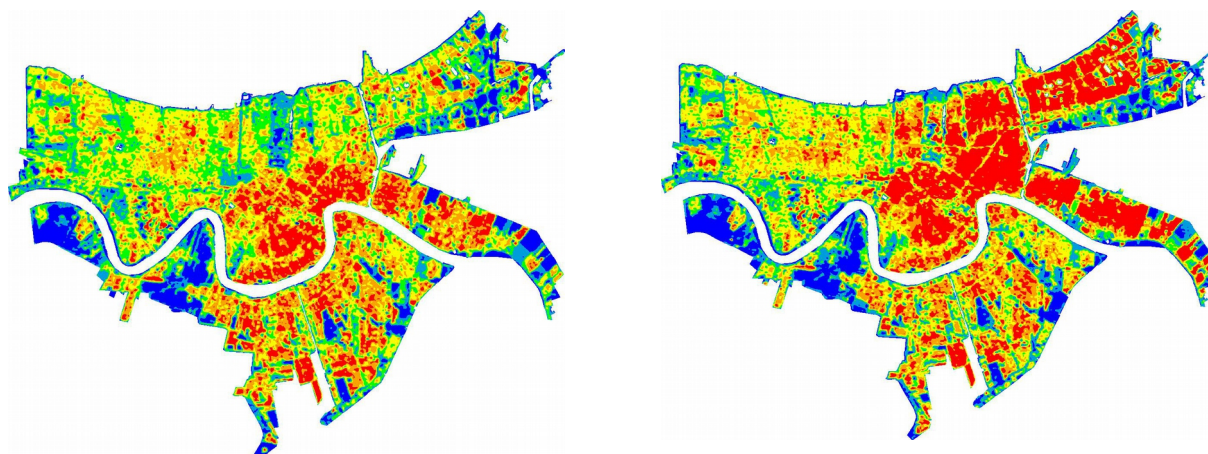


Figure 1. October 2003 and October 2005 LST images.

Table 1. October 2003 to October 2005 LST net increase change results.

Zone Class	Start Pixels	+/- °T Pixels	Total km ²	+/- °T km ²	+/- °T Change	% Change to Zone
6. Hot	66832	-15975	60.15	-14.38	-23.90%	19.57% to Zone 5
5. Very Warm	118365	41557	106.53	37.4	35.11%	35.11% to Zone 6
4. Warm	154280	53848	138.85	48.46	35.66%	18.26% to Zone 5
3. Cool-Warm	110290	50713	99.26	45.64	45.99%	29.86% to Zone 4
2. Cooler	74032	25548	66.63	22.93	35.42%	18.40% to Zone 3
1. Coolest	57098	16793	51.39	15.12	29.43%	22.54 % to Zone 2

Even though there were some hot areas that became cooler, the overall shift was upward in all the other temperature classes shown in Table 1. For example, in the lower left side of the AOI, there were some Zone 5 and 6 classes that became cooler. Upon visual inspection of DOQs, it was determined that these were grassy fields and areas of vegetative cover that were not affected by the persistent flooding that mainly occurred in Orleans and St. Bernard parishes. The vegetation in non-flooded areas may have benefited from the large amount of rain that came with the storm. The TM image was captured over one month after the impact of the storm, during a normally dry time of year, sufficient enough time for grass and some shrubs to regenerate. A reference table of the image histogram bin counts was created, showing the highest concentration was in Zone 6 for the 2005 image, which is apparent in the visualization of the data imagery, and the skewed nature of the histogram.

Finally in Table 2 below, the surface areas of the temperature zones for all the images were calculated. A dramatic increase of surface area in Zone 6 by 54.1 km², from 60.15 km² to 111.24 km², occurred from the year 2003 to 2005. The decrease of Zone 5 may have contributed to the increase in Zone 6 in 2005, the prior of which increased in 2006, along with a concomitant decrease in the latter for the same year. The data in the matrix shows a surface area increase in the hotter temperature zones, right after hurricane Katrina in 2005 (Zone 6), and the following two years (zone 5), which demonstrates the UHI effect was altered by the weather event, and then slowly returned to a similar, pre-storm state, before Hurricane Andrew. It appears Andrew may have impacted the UHI of the GNO area, but not to the extent of Katrina, the latter of which resulted in much more extensive flooding.

TM band 6 thermal image results were compared to classifications of the remaining Landsat bands (1-5,7) using the unsupervised method. 100 ISODATA classes were recoded to 6, except for two image dates that included two more classes: flooded areas and damaged trees. 150 iterations were performed at 0.997 convergence. Overall classification accuracy was 89.45%, and Kappa statistics was 0.8345. The accuracy of the COST atmospheric correction model was verified by comparing the accuracy of the classified images with an Internet-based, automated COST model builder (COST Maker).

Table 2. Histogram bin counts for all LST ISODATA images.

Date	Zone 1	Zone 2	Zone 3	Zone 4	Zone 5	Zone 6
1987	45.64 km ²	80.58 km ²	114.06 km ²	144.78 km ²	108.73 km ²	29.03 km ²
1992	48.82 km ²	85.34 km ²	127.37 km ²	95.37 km ²	109.91 km ²	55.99 km ²
1997	40.81 km ²	99.96 km ²	81.77 km ²	128.02 km ²	128.36 km ²	43.9 km ²
2002	40.55 km ²	98.52 km ²	87.6 km ²	125.39 km ²	127.36 km ²	43.38 km ²
2003	51.39 km ²	66.63 km ²	99.26 km ²	138.85 km ²	106.53 km ²	60.15 km ²
2005	48.23 km ²	69.91 km ²	67.47 km ²	132.1 km ²	90.86 km ²	114.24 km²
2006	53.39 km ²	71.06 km ²	90.58 km ²	103.6 km ²	157.96 km ²	46.22 km ²
2008	55.21 km ²	79.23 km ²	73.69 km ²	132.94 km ²	151.26 km ²	30.48 km ²
2010	51.51 km ²	73.08 km ²	97.52 km ²	139.02 km ²	136.98 km ²	24.69 km ²

124 enhanced indices were created from 31 images of all four seasons, plus image composites of combinations of the results, and indices that were modifications of others. For each of the 124 images, three raster image formats were created: 1) float images of the original spectral reflectance values (-0 to 1), rescaled images (0 to 1), and 8 bit rescale (0-255). The latter two formats were necessary for later experiments with certain composite indices that were rescaled to 8 bit. Although all of the 124 indices were capable of showing biomass, the best results were obtained using the NDMI enhancement because it most effectively detected the moisture in tree canopy with less background noise. Therefore it was used for all the selected images during this change detection procedure. The change to the vegetative biomass of the AOI is quite apparent in Figure 2. The profound loss of vegetation in Orleans Parish can be attributed to the flood waters that remained for several weeks.



Figure 2. NDMI image differences: 2003 to 2005, and 2005 to 2006.

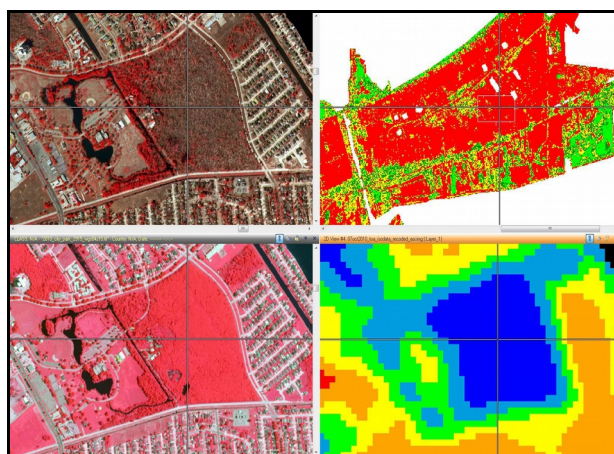


Figure 3. Clockwise from upper left: October 2005 DOQ, TM NDMI difference image 2003-2005, 2010 TM LST image, and July 2010 DOQ.

In Figure 3 above, the change of an urban forest in New Orleans East can be seen in the October 2005 DOQ and the July 2010 DOQ. The LST of the pixel in the cross-hairs is 24.0° C for 2003, 28.9° C for 2005, and 24.3° C for 2010. This demonstrates the resiliency of urban forests if left undisturbed after an impact as severe as a hurricane. If it is not converted into another subdivision, it will remain an *urban cool island* (UCI).

The the RGB method used for change detection, which is often used with NDVI (RGB-NDVI), utilizes three dates instead of two. After creating the composites, the next step was to classify the RGB-NDVI enhanced images using the unsupervised ISODATA method. 75 classes with a convergence of 0.997 at 170 iterations were the settings used. The 75 classes were recoded to 10 classes, and the results entered into tables for interpretation shown in Table 3. In Figure 4, one can see the large swath of magenta that dominates the right portion of the image, which signifies vegetation reduction from the year 2003 to 2005, and regeneration from 2005 to 2006. This is Hurricane Katrina's footprint, as seen in other enhanced images.

Table 3. RGB-NDVI change classification for years 2003 to 2005 and 2005 to 2006.

Display Color/Year Image Color	Red NDVI 2003	Green NDVI 2005	Blue NDVI 2006	Vegetation Change Interpretation
Red	High	Low	Low	Vegetation Reduction 2003-2005
Green	Low	High	Low	Regeneration 2003-2005; Reduction 2005-2006
Blue	Low	Low	High	Regeneration 2005-2006
Yellow	High	High	Low	Reduction 2005-2006
Magenta	High	Low	High	Reduction 2003-2005; Regeneration 2005-2006
Cyan	Low	High	High	Regeneration 2003-2005
Black	Low	Low	Low	No Change; Non-vegetation
Dark Gray	Low	Low	Low	No Change; Low Biomass
Medium Gray	Medium	Medium	Medium	No Change; Medium Biomass
Light Gray/White	High	High	High	No Change; High Biomass



Figure 4. RGB-NDVI composite: 2003-2005-2006. Hurricane Katrina's magenta footprint.

4. Conclusion

This study focused on using conventional remote sensing methods and data in order to determine the impact of a extreme, natural weather event on a human-induced climatic phenomenon. Hurricane Katrina and the flooding during its aftermath did have a direct impact on the UHI of the City. There is sufficient evidence derived from the data products to say there was an alteration of the local UHI effect, and that it was related to Hurricane Katrina's impact on the area. While urban forests were affected by high winds throughout the AOI, the most visible damage came from the stagnant flood water that remained for several weeks. The LST results derived from the TIR band of Landsat, and the thematic classifications enabled the measurement and characterization of the impact, as well as the dynamic nature of UHI in a constant state of flux. The spectral indices enabled measurements of vegetative health and abundance of biomass. Analysis of the enhancements found the vegetative cover was impacted, especially in the flooded areas, and visual representation of the enhanced data showed a pattern that matched the findings from the LST results. Furthermore, the vegetative cover did mostly return to the same areas, and analysis of two decades of imagery found a pattern of reduction and regeneration due to other storm impacts, though not as dramatic as the Katrina. A limitation of this study was the emphasis on a particular sensor platform and data set, and the requisite methods and techniques. The scope and nature of this investigation cannot possibly account for factors such as canopy and urban boundary layers, global-scale climate inputs and outputs, contribution of adjacent water bodies, and diurnal flux. Nevertheless, even with all of its faults and limitations, the Landsat TM sensor data was useful for characterizing the UHI effect at the regional and neighborhood scale of the AOI, and no other platform has the longest continuous record of Earth observations.

References:

- Cablk, M. E.; Michener, W. K.; Kjerfve, B.; Jensen, J. R. Impacts of Hurricane Hugo on Coastal Forest Assessment Using Landsat TM Data. **Journal of Remote Sensing**, v. 9, n. 2, p. 15-24, 1994.
- Chavez, P. S. Image-based atmospheric corrections-revisited and improved. **Photogrammetric Engineering and Remote Sensing**, v. 62, n. 9, p. 1025-1035, 1996.
- Foody, G. M. Status of land cover classification accuracy assessment. **Remote Sensing of Environment**, v. 80 n. 1, p. 185-201, 2002.
- Jiménez-Muñoz, J. C.; Sobrino, J. A.; Gillespie, A.; Sabol, D.; Gustafson, W. T. Improved land surface emissivities over agricultural areas using ASTER NDVI. **Remote Sensing of Environment**, v. 103 n. 4, p. 474-487, 2006.
- Lief, Aram P. **Spatial Analysis of Post-Hurricane Katrina Thermal Pattern and Intensity in Greater New Orleans: Implications for Urban Heat Island Research**. Dissertation (PhD in Urban Studies) - University of New Orleans, New Orleans. 2014.
- Oke, T. R. The energetic basis of the urban heat island. **Quarterly Journal of the Royal Meteorological Society**, v. 108, p. 1-24, 1982.
- Sader, S. A.; Bertrand, M.; Wilson, E. H. Satellite change detection of forest harvest patterns on an industrial forest landscape. **Forest Science**, v. 49, n.3, p. 341-353, 2003.
- Sobrino, J. A.; Jimenez-Muñoz, J. C.; Paolini, L. Land surface temperature retrieval from LANDSAT TM 5. **Remote Sensing of the Environment**, v. 90, p. 434-440, 2004.
- Wilson, E. H.; Sader, S. A. Detection of forest harvest type using multiple dates of Landsat TM imagery. **Remote Sensing of Environment**, v. 80, n. 3, p. 385-396, 2002.
- Yuan, F.; Bauer, M. E. Comparison of impervious surface area and normalized difference vegetation index as indicators of surface urban heat island effects in Landsat imagery. **Remote Sensing of Environment**, v. 106, n. 3, p. 375-386, 2007.